



HAL
open science

Temperature stability of proteins essential for the intracellular survival of *Mycobacterium tuberculosis*

Nathan A. Lack, Akane Kawamura, Elizabeth Fullam, Nicola Laurieri, Stacey Beard, Angela J. Russell, Dimitrios Evangelopoulos, Isaac Westwood, Edith Sim

► **To cite this version:**

Nathan A. Lack, Akane Kawamura, Elizabeth Fullam, Nicola Laurieri, Stacey Beard, et al.. Temperature stability of proteins essential for the intracellular survival of *Mycobacterium tuberculosis*. *Biochemical Journal*, 2009, 418 (2), pp.369-378. 10.1042/BJ20082011 . hal-00479108

HAL Id: hal-00479108

<https://hal.science/hal-00479108>

Submitted on 30 Apr 2010

HAL is a multi-disciplinary open access archive for the deposit and dissemination of scientific research documents, whether they are published or not. The documents may come from teaching and research institutions in France or abroad, or from public or private research centers.

L'archive ouverte pluridisciplinaire **HAL**, est destinée au dépôt et à la diffusion de documents scientifiques de niveau recherche, publiés ou non, émanant des établissements d'enseignement et de recherche français ou étrangers, des laboratoires publics ou privés.

Temperature stability of proteins essential for the intracellular survival of *Mycobacterium tuberculosis*

Nathan A. Lack^{*}, Akane Kawamura[†], Elizabeth Fullam^{*}, Nicola Laurieri^{*}, Stacey Beard^{*}, Angela J. Russell^{*‡}, Dimitrios Evangelopoulos^{*}, Isaac Westwood^{*} and Edith Sim^{*}

^{*}Department of Pharmacology, University of Oxford, Mansfield Road, Oxford OX1 3QT, UK

[†]Summit PLC, 91 Milton Park, Abingdon, OX14 4RY, UK

[‡]Department of Chemistry, University of Oxford, Mansfield Road, Oxford, OX1 3TA, UK

Running title: Characterization of HsaD and NAT from *M.tuberculosis*

Key words: Arylamine N-acetyltransferase, 2-hydroxy-6-oxo-6-phenylhexa-2,4-dienoic acid hydrolase, *Mycobacterium tuberculosis*, cholesterol, heat stability

Corresponding author: Edith Sim, edith.sim@pharm.ox.ac.uk
Fax: 0044 (0)1865 271884
Tel: 0044 (0)1865 271853

Abbreviations used: 4,9-DSHA, 4,5-9,10-diseco-3-hydroxy-5,9,17-trioxoandrosta-1(10),2-dien-4-oic acid; DTNB, 5, 5'-dithiobis 2-nitrobenzoic acid; HOPDA, 2-hydroxy-6-oxo-6-phenylhexa-2,4-dienoic acid; HsaD, 2-hydroxy-6-oxo-6-phenylhexa-2,4-dienoic acid hydrolase; NAT, arylamine N-acetyltransferase; MMNAT, arylamine N-acetyltransferase from *Mycobacterium marinum*; MM12TB3, arylamine N-acetyltransferase with domain one and two from *Mycobacterium marinum* and domain three from *Mycobacterium tuberculosis*; Ni-NTA, nickel nitrilotriacetic acid; TB12MM3, arylamine N-acetyltransferase with domain one and two from *Mycobacterium tuberculosis* and domain three from *Mycobacterium marinum*; TBNAT, arylamine N-acetyltransferase from *Mycobacterium tuberculosis*; TNB, 5-thio-2-nitrobenzoic acid

Abstract:

In *Mycobacterium tuberculosis* the genes *hsaD* (2-hydroxy-6-oxo-6-phenylhexa-2,4-dienoic acid hydrolase) and *nat* (arylamine N-acetyltransferase) are essential for survival inside of host macrophages. These genes act as an operon and have been suggested to be involved in cholesterol metabolism. However, the role of NAT in this catabolic pathway has not been determined. In an effort to better understand the function of these proteins, we have expressed, purified and characterized TBNAT and HsaD from *M. tuberculosis*. Both proteins demonstrated remarkable heat stability with TBNAT and HsaD retaining >95% of their activity following incubation at 60°C for 30 min. The first and second domain of TBNAT was demonstrated to be very important to the heat stability of the protein, as the transfer of these domains caused a dramatic reduction in the heat stability. The specific activity of TBNAT was tested against a broad range of acyl CoA cofactors using hydralazine as a substrate. TBNAT was found to be able to utilize not just acetyl CoA, but also *n*-propionyl CoA and acetoacetyl CoA, though at a slower rate. As propionyl CoA is a product of cholesterol catabolism, we propose NAT could have a role in the utilization of this important cofactor.

Introduction

Despite over one hundred years of research, *Mycobacterium tuberculosis*, a causative agent of tuberculosis, remains one of the leading causes of death by bacterial infection. While the pathogenesis of the bacterium is extremely complex, the success of this organism has largely been attributed to its ability to reside intracellularly in macrophages, which allows the bacteria to avoid the threat of the host immune response [1-3]. Unable to suppress the bacterial infection, the host immune system encases the infected macrophages into dense granuloma structures which are believed to be metabolically barren environments with low oxygen and poor nutrient availability [4]. Yet, despite these harsh conditions, *M. tuberculosis* has been demonstrated to survive over 40 years within a granuloma [5, 6]. During this long-term survival, the bacterium appears to be metabolically active, suggesting that *M. tuberculosis* must utilize alternative nutrients [7]. As such, further study of nutrient metabolism in *M. tuberculosis* would greatly assist the understanding of long-term persistence and bacterial pathogenesis.

Arylamine N-acetyltransferase (NAT) is a cytosolic protein which transfers an acetyl group from acetyl-CoA to an arylamine species [8]. NAT enzymes have been identified in numerous eukaryotic and prokaryotic species, including *Mycobacterium smegmatis*, *Mycobacterium bovis* BCG and *M. tuberculosis* [9, 10]. Within *M. tuberculosis*, NAT is found in a five-gene operon that contains the enzymes *hsaA* (Rv3570c), *hsaD* (Rv3569c), *hsaC* (Rv3568c), *hsaB* (Rv3567c) and *nat* (Rv3566) (**Figure 1**) [11]. Individual genetic knockouts of *hsaD*, *hsaA* and *nat* are unable to survive within macrophages, highlighting the importance of this operon [12, 13]. The expression of this operon is controlled by the TetR-like repressor KstR, which is believed to be involved in lipid metabolism [14]. Supporting this role, homologues of the genes *hsaA*, *hsaD*, *hsaC* and *hsaB* in *Rhodococcus* RHA1 have been demonstrated to be involved in the *meta*-cleavage of cholesterol (**Figure 2**) [15]. The role of NAT in cholesterol degradation remains unresolved, with no direct links between the established enzymic reactions of NAT and cholesterol metabolism. While the exact role of intracellular cholesterol *in vivo* is unknown, recent studies have demonstrated that *M. tuberculosis* can utilize cholesterol as a carbon source and that cholesterol could be important for bacterial persistence [16, 17]. Furthermore, it has been reported in humans and mice with late-stage tuberculosis that large amounts of cholesterol can become concentrated in alveoli and that many bacteria will closely associate with lipid droplets in the necrotic foci of caseating granulomas [18-21].

2-Hydroxy-6-oxo-6-phenylhexa-2,4-dienoic acid hydrolase (HsaD) is a cytosolic carbon-carbon hydrolase that can catalyze the cleavage of the cholesterol metabolite 4,5,9,10-diseco-3-hydroxy-5,9,17-trioxoandrosta-1(10),2-dien-4-oic acid (4,9-DSHA) into 9,17-dioxo-1,2,3,4,10,19-hexanorandrostan-5-oic acid and 2-hydroxyhexa-2,4-dienoic acid [15, 22]. While the enzyme was originally annotated as being involved in biphenyl metabolism, recent work has demonstrated that HsaD has preferential selectivity for 4,9-DSHA as a substrate over the biphenyl metabolite 2-hydroxy-6-oxo-6-phenylhexa-2,4-dienoic acid (HOPDA) [15]. Furthermore, in the structure of HsaD there is a considerably larger active site than that found in homologous enzymes that are involved in biphenyl

degradation, which may provide the necessary space to fit the considerably larger cholesterol metabolite 4,9 DSHA [23].

To better understand the role of the proteins encoded by this essential operon, we have produced recombinant HsaD and NAT from *M. tuberculosis* and in this work describe their characterization.

Materials and Methods

Materials

Unless specifically stated, all chemicals and reagents were purchased from Sigma Aldrich (Poole, Dorset, UK). All enzymes were purchased from Promega (UK Ltd., Southampton, UK) or New England Biolabs (UK LTD Hitchin, UK).

Chemical synthesis of 2-hydroxy-6-oxo-6-phenylhexa-2,4-dienoic acid (HOPDA)

HOPDA was produced synthetically using a chemical route modified from that reported by Speare et al. [24]. The experimental protocol and chemical products are described in the **Supplementary Data**. The molar extinction coefficient for HOPDA was calculated in 100mM phosphate buffer (pH 7.4) with 20mM NaCl and determined to be $13.2 \text{ mM}^{-1} \text{ cm}^{-1}$. The calculated molar extinction coefficient is similar to previous published values [25].

Heterologous expression and purification of *M. tuberculosis* NAT, *Mycobacterium marinum* NAT and chimeric proteins

NAT from *M. tuberculosis* (TBNAT), *Mycobacterium marinum* (MMNAT) and the chimeric TBNAT/MMNAT proteins were produced as previously described [10, 26, 27].

NAT enzyme activity measurement

The rate of coenzyme A (CoA) formation was determined spectrophotometrically using the colourimetric agent 5, 5'-dithiobis 2-nitrobenzoic acid (Ellman's reagent, DTNB) as previously described [28]. Briefly, the production of the coloured 5-thio-2-nitrobenzoic acid (TNB) was assayed at 405nm following the reaction of DTNB with the free thiol-CoA that is formed during the enzymatic reaction. The specific activity of TBNAT with various acyl CoA species was determined by incubating TBNAT (0.75µg) in the presence of 500µM hydralazine and different acyl CoA species (400 µM) in assay buffer (20 mM Tris-HCl, pH 8.0) with 0.5% DMSO at 37°C. Apparent kinetic parameters were calculated using variable concentrations of acyl CoA (20 to 640µM) with a fixed concentration of hydralazine (500µM) and NAT enzyme (0.5µg/ml NAT in 20mM Tris-HCl, pH 8.0 with 0.5% DMSO). The time was adjusted such that a linear initial rate was measured which corresponded to a change in absorbance of at least 0.2 absorbance units at 405nm. The kinetic constants were calculated by hyperbolic fit to the initial rate.

Cloning, heterologous expression and purification of HsaD

The gene encoding 2-hydroxy-6-oxo-6-phenylhexa-2,4-dienoic acid hydrolase (*rv3569c*) from *M. tuberculosis* H37Rv was PCR amplified from gDNA (For 5'-**TTCATATGATGACAGCTACCGAGGAA**-3', Rev 5'-**GCGGATCCTCATCTGCCACCTCC**-3'), digested with *NdeI/BamHI* and cloned into

pET28b(+). Following sequencing, the *hsaD* insert was digested with *XbaI/HindIII* from pET28b(+)-*hsaD*, removing the gene with a hexa-histidine tag. This fragment was gel purified and cloned into pVLT31 to yield the plasmid pVLT31-*hsaD_H6*. Following confirmation of the sequence, the plasmid was electroporated into electrocompetent *Pseudomonas putida* strain KT2442.

P. putida containing pVLT31-*hsaD_H6* was grown at 30°C in LB medium supplemented with 10 µg/ml rifampin and 12.5 µg/ml tetracycline to an absorbance of 1.0 at 600nm and induced with 1mM IPTG overnight. The culture was harvested (6,000 x g, 20min, 4°C) and the pellet was resuspended in 25ml of lysis buffer (100mM phosphate buffer pH 7.4, 25mM imidazole, 25 µg/ml DNase I, 200µg/ml lysosyme, 1mM pefabloc). The bacteria were lysed by sonication at 4°C and centrifuged at 16,000 x g for 20 minutes. The lysate was filtered through a 0.2µm filter and run on a Nickel-NTA (nitrilotriacetic acid) column (2ml resin/L of bacterial culture). The column was washed sequentially with 2 column volumes (4ml) of 100mM phosphate buffer (pH 7.4) containing the following concentrations of imidazole: 25, 50, 100, 250mM. The fractions were collected and a sample of each (5µl) was run on a 12% SDS-PAGE. The fractions which contained HsaD purified to apparent homogeneity were dialyzed into 100mM sodium phosphate buffer pH 7.4 20mM NaCl and concentrated with an Amicon Ultra concentrator (Millipore) to give a final yield of 10-20mg of pure HsaD/L of bacterial culture.

The enzymatic activity of HsaD was measured by incubating 45µl of 1.3µM purified HsaD in 100mM phosphate buffer (pH 7.4) with 20mM NaCl with 5µl HOPDA (45-460µM) and monitoring the decrease in absorbance of HOPDA at 450nm over 180 sec (Sunrise, Tecan). The K_m^{app} and V_{max}^{app} were determined by hyperbolic fit to the initial rate.

Physical properties of the enzymes

Analytical ultracentrifugation

Purified HsaD (0.5mg/ml) was centrifuged at 4000, 5500, 7000 and 10000 rpm for 10hrs at 20°C and then scanned at 280nm across the centrifuge rotor (Beckman Optima XL-A). Following the completion of the first scan, the sample was centrifuged for an additional 2hrs and then scanned at 280nm across the centrifuge rotor to confirm that the sample had reached equilibrium. The absorbance vs. radii was fitted to a first order exponential curve using the software suite Ultraspin (<http://ultraspin.mrc-cpe.cam.ac.uk>).

Circular Dichroism

Purified HsaD (5µM) in 100mM sodium phosphate buffer (pH 7.4) with 20mM NaCl was incubated at a range of temperatures (20-85°C as determined by the internal temperature probe) for 240 seconds. Following incubation the circular dichroism of the sample was measured from 200-260nm on a Jasco J720 spectropolarimeter. The temperature of the sample was measured with an internal temperature probe.

Effect of heat on protein activity

Each of the protein samples (HsaD, TBNAT, MMNAT, MM12TB3, TB12MM3) were incubated at temperatures from 20-85°C for 30min, placed on ice for 5 min, centrifuged at 12,000 $x g$ for five minutes and then assayed for activity.

Results

Purification and characterization of TBNAT with respect to the acyl donor

TBNAT was expressed as a his-tagged protein and purified with a nickel-NTA resin to apparent homogeneity. Previous studies have demonstrated that TBNAT can acetylate hydralazine at a greater rate than any other substrate tested [27, 29]. As such, various coenzyme A derivatives were tested as cofactors of TBNAT using hydralazine as a substrate (**Figure 3**). The hydrolysis of the thiol ester was readily measurable with *n*-propionyl CoA and acetoacetyl CoA but at a slower rate than with acetyl CoA. The K_m^{app} was determined and found to be 0.56 ± 0.03 mM for acetyl-CoA and 0.29 ± 0.02 mM for *n*-propionyl CoA. The K_m^{app} acetoacetyl-CoA was found to be greater than 0.6mM and could not be determined accurately due to the low rate of reaction.

HsaD production and purification

Numerous attempts to express HsaD using *E.coli* and T7 polymerase expression plasmids have been unsuccessful. Therefore, an alternative expression system was utilized, in which the gene encoding HsaD (with a hexa-histidine tag) was digested from the previously generated pET28b(+)-*hsaD* construct and cloned into the broad-host expression plasmid pVLT31 [30]. This newly generated construct was then cloned into *Pseudomonas putida* KT2442 and the expression conditions were optimized. The highest yields of HsaD were obtained when bacteria was grown in LB with 12.5 μ g/ml tetracycline and 10 μ g/ml rifamycin at 30°C to an $OD_{600nm}=1.0$ and then induced with 1mM IPTG overnight. The presence of the hexa-histidine tag introduced from pET28b(+) allowed for one-step purification using Ni-NTA resin, purifying the enzyme to apparent homogeneity as determined by SDS-PAGE (**Figure 4**). The molecular weight of the protein was determined by SDS-PAGE to be 33.8kDa, which agrees with the predicted molecular weight of HsaD with a hexa-histidine tag. The identity of HsaD was confirmed by matrix-assisted laser desorption ionisation time-of-flight mass spectroscopy (MASCOT score >8300). This expression protocol produced 10-20mg of purified HsaD/L of bacterial culture.

Characterisation of recombinant HsaD

The molecular weight of HsaD in solution was determined by analytic ultracentrifugation equilibrium sedimentation (**Supplementary Figure 1**). The molecular weight of HsaD was calculated to be 132 ± 9 kDa ($n=16$) suggesting that HsaD (33.75kDa) forms a tetramer in solution. Using increasing concentrations of HOPDA the enzyme kinetics of HsaD were studied. From this, the K_m^{app} of HOPDA was calculated to be 0.23 ± 0.02 mM, the V_{max}^{app} 3.5 ± 0.2 mM $min^{-1} mg^{-1}$, the K_{cat} $0.25 s^{-1}$ and the K_{cat}/K_m^{app} $1129 s^{-1} M^{-1}$. The K_m^{app} of HOPDA was not significantly different between HsaD with (0.23 ± 0.02 mM) and without a hexa-histidine tag (0.24 ± 0.05 mM).

Thermal Stability

Both TBNAT and HsaD demonstrated very high heat stability (**Figure 5A and 6A**). With TBNAT, the enzyme begins to lose activity following incubation at temperatures higher than 60°C and was completely inactivated at 75°C (**Figure 5A**). This heat stability is not found in any other bacterial or mammalian NATs previously characterised [31-33]. A lower heat stability was found in NAT from *M. marinum*, with the enzyme losing all activity following incubation at 50°C (**Figure 5B**). The first and second domains of TBNAT appear to strongly influence the heat stability of the protein (**Figure 5B**). The transfer of domain one and two from MMNAT to TBNAT (MM12TB3) considerably decreased the enzymatic heat stability (**Figure 5B**). In contrast with the chimeric protein in which only the third domain from MMNAT is transferred to TBNAT (TB12MM3), the temperature stability profile is very similar to TBNAT itself (**Figure 5A**).

The effect of temperature on HsaD stability was assayed by studying both enzymic activity and circular dichroism. When the protein was heated, the CD spectrum associated with the protein's alpha helices (as identified by the signal at 220nm) diminished dramatically across a temperature range of 65 to 70°C (**Figure 6A**). When the protein was incubated at 65±0.4°C (as determined by the sample probe), the alpha helices unfolded in a linear time-dependent manner (**Figure 6B**). The co-operative unfolding of the protein occurred over the same temperature range when assessed by enzymatic activity as when assessed by loss of circular dichroism signal at 220nm (**Figure 6A**). Hydrolytic activity was significantly decreased following incubation at 70°C but was only marginally affected by incubation at 60°C for 30 min (**Figure 6A**). Increasing concentrations of NaCl did not alter the heat stability of HsaD (**Figure 6C**). The heat stability of HsaD was not altered by the presence or absence of a hexa-histidine tag (data not shown).

Discussion

Previous work has demonstrated that the five predicted open reading frames (*Rv3566c-Rv3570c*), which include the genes encoding HsaD and TBNAT, are expressed as a single mRNA transcript (**Figure 1**) [11]. As these genes act as an operon, it is likely that they support a coordinated function. In order to better understand the role of this operon in *M. tuberculosis*, we have cloned, expressed and characterized HsaD and TBNAT.

Attempts to express soluble HsaD using T7 polymerase expression systems were unsuccessful [34]. It was only when the expression plasmid pVLT31 [30] was used that soluble HsaD was expressed. The introduction of a hexa-histidine tag into the expression plasmid greatly assisted in protein purification. HsaD was demonstrated by analytical ultracentrifugation to form a tetramer in solution, which is consistent with the behaviour of other *meta*-cleavage hydrolases [35-37] and agrees with the predicted oligomerization state from the crystal structure of HsaD [23].

The high enzymatic heat stability of TBNAT has not been found in the NAT enzymes from any other species, including the closely related organisms *Mycobacterium smegmatis* [31] and *M. marinum* (**Figure 5B**). NAT from *M. smegmatis* [38] and *M. marinum* [26] have been used as models of the more difficult to express TBNAT. The first and second domains of NAT from *M. tuberculosis* [9] appear to contribute strongly

to the thermal stability of the protein, with the transfer of domain one and two from MMNAT to TBNAT causing a dramatic reduction in the heat stability (**Figure 5B**). In an effort to identify residues which may be important to the heat stability of TBNAT, the primary sequence of the first and second domain of NAT from *M. smegmatis* and *M. marinum* was compared with the first and second domain of TBNAT (**Figure 7A**). Fourteen residues were identified that were present in both NAT from *M. smegmatis* and *M. marinum* but not TBNAT. The location of these amino acid differences were mapped onto the structure of MMNAT (**Figure 7B**). Interestingly, twelve of these fourteen amino acid residues were found to be surface exposed on MMNAT (**Figure 7C+D**) [26]. In TBNAT ten of the changed residues involve a change to a more hydrophobic residue, two involve substitution of an alanine residue by proline (residues 54 and 106) and a further proline substitution for a glutamine is found in TBNAT (residue 148). In two cases a negatively charged residue has been replaced by an uncharged residue (Glu 55 replaced by Gln, Glu 63 replaced by Leu and Glu 172 replaced by Thr) where the residues are the same in both *M. marinum* and *M. smegmatis* NAT proteins (**Figure 7A**). Previous studies of cold shock proteins from *Bacillus* species has demonstrated that just a few surface exposed residues can play a major role in the protein's heat stability [39].

HsaD displayed a strong correlation between protein denaturation and a decrease in enzymatic activity (**Figure 6A**). In addition, the temperature stability of HsaD was not significantly affected by increasing ionic strengths (**Figure 6C**), suggesting that hydrophobic interactions may be important in stabilizing the protein. This is supported with evidence from the crystal structure of HsaD, with the highest concentration of surface exposed hydrophobic amino acids in a region where the protein forms a tetrameric core. The maximal temperature that HsaD can tolerate before there is any significant loss of activity is 60°C. This is comparable to several *meta*-cleavage hydrolases expressed in mesophilic bacteria, including BphD from *Rhodococcus* RHA1 (65°C) [40], ThnD from *Sphingomonas macrogoltabidus* strain TFA (65°C) [41] and CarC from *Pseudomonas resinovorans* strain CA10 (58°C) [42] (**Table 1**). In contrast, a second group of *meta*-cleavage hydrolases, including TodF from *Pseudomonas putida* (45°C) [43] and CumD from *Pseudomonas fluorescens* IP01 (48°C) [44], have a lower maximal temperature that can be tolerated before there is a loss of activity (**Table 1**). Comparison of the primary sequences of these two groups of *meta*-cleavage hydrolases does not identify any specific amino acids which could contribute to the heat stability of the protein. This may well be expected as these *meta*-cleavage hydrolases share a relatively low sequence similarity (23-32% identity to HsaD) (**Figure 8A**) and yet have a very similar structural fold (r.m.s. 1.29-1.81 Å alignment of HsaD to BphD, CarC and CumD, respectively) (**Figure 8B**).

The genes which encode HsaD and TBNAT have been demonstrated to be critical for intracellular survival of *M. tuberculosis* in host macrophages [12, 13]. During the initial bacterial infection there is a marked increase in internal temperature as a defence mechanism against the pathogen. The enzymatic heat stability of HsaD and TBNAT may prevent the inactivation of these proteins during the initial infection as both proteins are completely active at temperatures greater than 50°C. Whilst the intracellular temperature, even during the macrophage respiratory burst, is unlikely to reach 45°C, many NAT

enzymes will lose >50% of their activity at this temperature. In contrast, NAT and HsaD from *M. tuberculosis* will be completely active at this temperature creating a “margin of safety” for these essential enzymes.

The proposed pathway of cholesterol degradation contains two independent metabolic routes, where one pathway is involved in the removal and oxidation of the C17 acyl chain, while another degrades the four-ring cholesterol skeleton (**Figure 2**) [15, 22, 45, 46]. Previous studies have demonstrated that products of this operon (HsaA, HsaB, HsaC and HsaD) are likely to have a role in the oxidation and *meta*-cleavage of the cholesterol skeleton [15]. However, the role of TBNAT, which is encoded in the same operon, does not easily fit into the proposed degradation pathway of the four-ring cholesterol skeleton. Interestingly, the second metabolic pathway involved in the degradation of the C17 acyl chain will yield one molecule of acetyl CoA and two molecules of *n*-propionyl CoA per cholesterol molecule (**Figure 2**) [15, 46, 47]. Given that TBNAT can utilize both *n*-propionyl and acetyl CoA donors (**Figure 3**), it is proposed that TBNAT could have a role in the utilization and regulation of these CoA species. The utilization of *n*-propionyl CoA is doubly important to bacterial survival, as *n*-propionyl CoA can be toxic to the bacteria at high concentrations and yet acts as a key precursor in lipid biosynthetic pathways [48]. The K_m^{app} of acetyl CoA and propionyl CoA with TBNAT are of the same order of magnitude, though the rate of the enzymatic reaction with propionyl CoA is considerably less. It remains to be determined whether this mechanism is effective *in vivo*, but it provides a hypothesis for the functional integration of the operon. Thus as indicated in **Figure 1**, TBNAT may act to promote propionyl CoA and acetyl CoA usage and homeostasis for cell wall synthesis, with cholesterol providing the fuel both via the degradation of the acyl side chain and the *meta*-cleavage of the sterol rings. Given the importance of cholesterol for intracellular survival of *M. tuberculosis* [16, 17] these enzymes are an important focus for further studies.

Acknowledgements

We are grateful to the Wellcome Trust for financial support. NAL is funded by the Natural Science and Engineering Council of Canada and Linacre College, Oxford. We thank Lindsay Eltis for generously donating the plasmid pVLT31.

- 1 Russell, D. G. (2001) *Mycobacterium tuberculosis*: here today, and here tomorrow. *Nat Rev Mol Cell Biol.* **2**, 569-577
- 2 Ferrari, G., Langen, H., Naito, M. and Pieters, J. (1999) A coat protein on phagosomes involved in the intracellular survival of mycobacteria. *Cell.* **97**, 435-447
- 3 Stewart, G. R., Robertson, B. D. and Young, D. B. (2003) Tuberculosis: a problem with persistence. *Nat Rev Microbiol.* **1**, 97-105
- 4 Russell, D. G. (2007) Who puts the tubercle in tuberculosis? *Nat Rev Microbiol.* **5**, 39-47
- 5 Wayne, L. G. and Sohaskey, C. D. (2001) Nonreplicating persistence of *Mycobacterium tuberculosis*. *Annu Rev Microbiol.* **55**, 139-163
- 6 Marks, G. B., Bai, J., Simpson, S. E., Sullivan, E. A. and Stewart, G. J. (2000) Incidence of tuberculosis among a cohort of tuberculin-positive refugees in Australia: reappraising the estimates of risk. *Am J Respir Crit Care Med.* **162**, 1851-1854
- 7 Fenhalls, G., Stevens, L., Moses, L., Bezuidenhout, J., Betts, J. C., Helden Pv, P., Lukey, P. T. and Duncan, K. (2002) In situ detection of *Mycobacterium tuberculosis* transcripts in human lung granulomas reveals differential gene expression in necrotic lesions. *Infect Immun.* **70**, 6330-6338
- 8 Sim, E., Westwood, I. and Fullam, E. (2007) Arylamine N-acetyltransferases. *Expert Opin Drug Metab Toxicol.* **3**, 169-184
- 9 Payton, M., Mushtaq, A., Yu, T. W., Wu, L. J., Sinclair, J. and Sim, E. (2001) Eubacterial arylamine N-acetyltransferases - identification and comparison of 18 members of the protein family with conserved active site cysteine, histidine and aspartate residues. *Microbiology.* **147**, 1137-1147
- 10 Upton, A. M., Mushtaq, A., Victor, T. C., Sampson, S. L., Sandy, J., Smith, D. M., van Helden, P. V. and Sim, E. (2001) Arylamine N-acetyltransferase of *Mycobacterium tuberculosis* is a polymorphic enzyme and a site of isoniazid metabolism. *Mol Microbiol.* **42**, 309-317
- 11 Anderton, M. C., Bhakta, S., Besra, G. S., Jeavons, P., Eltis, L. D. and Sim, E. (2006) Characterization of the putative operon containing arylamine N-acetyltransferase (*nat*) in *Mycobacterium bovis* BCG. *Mol Microbiol.* **59**, 181-192
- 12 Bhakta, S., Besra, G. S., Upton, A. M., Parish, T., Sholto-Douglas-Vernon, C., Gibson, K. J., Knutton, S., Gordon, S., DaSilva, R. P., Anderton, M. C. and Sim, E. (2004) Arylamine N-acetyltransferase is required for synthesis of mycolic acids and complex lipids in *Mycobacterium bovis* BCG and represents a novel drug target. *J Exp Med.* **199**, 1191-1199
- 13 Rengarajan, J., Bloom, B. R. and Rubin, E. J. (2005) Genome-wide requirements for *Mycobacterium tuberculosis* adaptation and survival in macrophages. *Proc Natl Acad Sci U S A.* **102**, 8327-8332
- 14 Kendall, S. L., Withers, M., Soffair, C. N., Moreland, N. J., Gurcha, S., Sidders, B., Frita, R., Ten Bokum, A., Besra, G. S., Lott, J. S. and Stoker, N. G. (2007) A highly conserved transcriptional repressor controls a large regulon involved in lipid degradation in *Mycobacterium smegmatis* and *Mycobacterium tuberculosis*. *Mol Microbiol.* **65**, 684-699
- 15 Van der Geize, R., Yam, K., Heuser, T., Wilbrink, M. H., Hara, H., Anderton, M. C., Sim, E., Dijkhuizen, L., Davies, J. E., Mohn, W. W. and Eltis, L. D. (2007) A gene cluster encoding cholesterol catabolism in a soil actinomycete provides insight into

- Mycobacterium tuberculosis survival in macrophages. Proc Natl Acad Sci U S A. **104**, 1947-1952
- 16 Pandey, A. K. and Sasseti, C. M. (2008) Mycobacterial persistence requires the utilization of host cholesterol. Proc Natl Acad Sci U S A. **105**, 4376-4380
- 17 Brzostek, A., Dziadek, B., Rumijowska-Galewicz, A., Pawelczyk, J. and Dziadek, J. (2007) Cholesterol oxidase is required for virulence of Mycobacterium tuberculosis. FEMS Microbiol Lett. **275**, 106-112
- 18 Cardona, P. J., Gordillo, S., Diaz, J., Tapia, G., Amat, I., Pallares, A., Vilaplana, C., Ariza, A. and Ausina, V. (2003) Widespread bronchogenic dissemination makes DBA/2 mice more susceptible than C57BL/6 mice to experimental aerosol infection with Mycobacterium tuberculosis. Infection & Immunity. **71**, 5845-5854
- 19 Dunn, P. L. and North, R. J. (1996) Persistent infection with virulent but not avirulent Mycobacterium tuberculosis in the lungs of mice causes progressive pathology. Journal of Medical Microbiology. **45**, 103-109
- 20 Hunter, R. L., Olsen, M., Jagannath, C. and Actor, J. K. (2006) Trehalose 6,6'-dimycolate and lipid in the pathogenesis of caseating granulomas of tuberculosis in mice. American Journal of Pathology. **168**, 1249-1261
- 21 Pagel W, P. W. (1925) Zur Histochemie der Lungentuberkulose, mit besonderer Berücksichtigung der Fettsubstanzen und Lipide. (Fat and lipid content to tuberculosis tissue. Histochemical investigation). Virchows Arch Pathol Anat. **256**, 11
- 22 Horinouchi, M., Hayashi, T., Koshino, H., Kurita, T. and Kudo, T. (2005) Identification of 9,17-dioxo-1,2,3,4,10,19-hexanorandrostanoic acid, 4-hydroxy-2-oxohexanoic acid, and 2-hydroxyhexa-2,4-dienoic acid and related enzymes involved in testosterone degradation in Comamonas testosteroni TA441. Appl Environ Microbiol. **71**, 5275-5281
- 23 Lack, N., Lowe, E. D., Liu, J., Eltis, L. D., Noble, M. E., Sim, E. and Westwood, I. M. (2008) Structure of HsaD, a steroid-degrading hydrolase, from Mycobacterium tuberculosis. Acta Crystallogr Sect F Struct Biol Cryst Commun. **64**, 2-7
- 24 Speare, D. M., Fleming, S. M., Beckett, M. N., Li, J. J. and Bugg, T. D. (2004) Synthetic 6-aryl-2-hydroxy-6-ketohexa-2,4-dienoic acid substrates for C-C hydrolase BphD: investigation of a general base catalytic mechanism. Org Biomol Chem. **2**, 2942-2950
- 25 Mukerjee-Dhar, G., Shimura, M., Miyazawa, D., Kimbara, K. and Hatta, T. (2005) bph genes of the thermophilic PCB degrader, Bacillus sp. JF8: characterization of the divergent ring-hydroxylating dioxygenase and hydrolase genes upstream of the Mn-dependent BphC. Microbiology. **151**, 4139-4151
- 26 Fullam, E., Westwood, I. M., Anderton, M. C., Lowe, E. D., Sim, E. and Noble, M. E. (2008) Divergence of cofactor recognition across evolution: coenzyme A binding in a prokaryotic arylamine N-acetyltransferase. Journal of molecular biology. **375**, 178-191
- 27 Fullam, E., Kawamura, A., Wilkinson, H., Westwood, I. M. and Sim, E. (2008) Investigation of MMNAT and mutants: Comparison of the arylamine N-acetyltransferase from Mycobacterium marinum and Mycobacterium tuberculosis. Protein Expression & Purification. *under review*

- 28 Brooke, E. W., Davies, S. G., Mulvaney, A. W., Pompeo, F., Sim, E. and Vickers, R. J. (2003) An approach to identifying novel substrates of bacterial arylamine N-acetyltransferases. *Bioorg Med Chem.* **11**, 1227-1234
- 29 Sikora, A. L., Frankel, B. A. and Blanchard, J. S. (2008) Kinetic and Chemical Mechanism of Arylamine N-Acetyltransferase from *Mycobacterium tuberculosis*. *Biochemistry.* **17**, 17
- 30 de Lorenzo, V., Eltis, L., Kessler, B. and Timmis, K. N. (1993) Analysis of *Pseudomonas* gene products using *lacIq*/*P*_{trp}-*lac* plasmids and transposons that confer conditional phenotypes. *Gene.* **123**, 17-24
- 31 Kawamura, A., Sandy, J., Upton, A., Noble, M. and Sim, E. (2003) Structural investigation of mutant *Mycobacterium smegmatis* arylamine N-acetyltransferase: a model for a naturally occurring functional polymorphism in *Mycobacterium tuberculosis* arylamine N-acetyltransferase. *Protein expression and purification.* **27**, 75-84
- 32 Sinclair, J. C., Sandy, J., Delgoda, R., Sim, E. and Noble, M. E. (2000) Structure of arylamine N-acetyltransferase reveals a catalytic triad. *Nat Struct Biol.* **7**, 560-564
- 33 Kawamura, A., Graham, J., Mushtaq, A., Tsiftoglou, S. A., Vath, G. M., Hanna, P. E., Wagner, C. R. and Sim, E. (2005) Eukaryotic arylamine N-acetyltransferase. Investigation of substrate specificity by high-throughput screening. *Biochem Pharmacol.* **69**, 347-359
- 34 Anderton, M. C. (2005) Characterization of the putative operon containing arylamine N-acetyltransferase (*nat*) in mycobacteria. In *Pharmacology ed.* (eds.). p. 188, University of Oxford, Oxford
- 35 Seah, S. Y., Ke, J., Denis, G., Horsman, G. P., Fortin, P. D., Whiting, C. J. and Eltis, L. D. (2007) Characterization of a C-C bond hydrolase from *Sphingomonas wittichii* RW1 with novel specificities towards polychlorinated biphenyl metabolites. *Journal of Bacteriology.* **189**, 4038-4045
- 36 Horsman, G. P., Ke, J., Dai, S., Seah, S. Y., Bolin, J. T. and Eltis, L. D. (2006) Kinetic and structural insight into the mechanism of BphD, a C-C bond hydrolase from the biphenyl degradation pathway. *Biochemistry.* **45**, 11071-11086
- 37 Nandhagopal, N., Yamada, A., Hatta, T., Masai, E., Fukuda, M., Mitsui, Y. and Senda, T. (2001) Crystal structure of 2-hydroxyl-6-oxo-6-phenylhexa-2,4-dienoic acid (HPDA) hydrolase (BphD enzyme) from the *Rhodococcus* sp. strain RHA1 of the PCB degradation pathway. *Journal of molecular biology.* **309**, 1139-1151
- 38 Sandy, J., Mushtaq, A., Kawamura, A., Sinclair, J., Sim, E. and Noble, M. (2002) The structure of arylamine N-acetyltransferase from *Mycobacterium smegmatis*--an enzyme which inactivates the anti-tubercular drug, isoniazid. *Journal of molecular biology.* **318**, 1071-1083
- 39 Perl, D., Mueller, U., Heinemann, U. and Schmid, F. X. (2000) Two exposed amino acid residues confer thermostability on a cold shock protein.[see comment]. *Nature Structural Biology.* **7**, 380-383
- 40 Hatta, T., Shimada, T., Yoshihara, T., Yamada, A., Masai, E., Fukuda, M. and Kiyohara, H. (1998) Meta-Fission Product Hydrolases from a Strong PCB Degradator *Rhodococcus* sp. RHA1. *Journal of Fermentation and Bioengineering.* **85**, 174-179(176)
- 41 Hernaez, M. J., Andujar, E., Rios, J. L., Kaschabek, S. R., Reineke, W. and Santero, E. (2000) Identification of a serine hydrolase which cleaves the alicyclic ring of tetralin. *Journal of Bacteriology.* **182**, 5448-5453

- 42 Riddle, R. R., Gibbs, P. R., Willson, R. C. and Benedik, M. J. (2003) Purification and properties of 2-hydroxy-6-oxo-6-(2'-aminophenyl)hexa-2,4-dienoic acid hydrolase involved in microbial degradation of carbazole. *Protein Expression & Purification*. **28**, 182-189
- 43 Bayly, R. C. and di Berardino, D. (1978) Purification and properties of 2-hydroxy-6-oxo-2,4-heptadienoate hydrolase from two strains of *Pseudomonas putida*. *Journal of Bacteriology*. **134**, 30-37
- 44 Saku, T., Fushinobu, S., Jun, S. Y., Ikeda, N., Nojiri, H., Yamane, H., Omori, T. and Wakagi, T. (2002) Purification, characterization, and steady-state kinetics of a meta-cleavage compound hydrolase from *Pseudomonas fluorescens* IPO1. *J Biosci Bioeng*. **93**, 568-574
- 45 Sih, C. J., Lee, S. S., Tsong, Y. Y. and Wang, K. C. (1966) Mechanisms of steroid oxidation by microorganisms. 8. 3,4-Dihydroxy-9,10-secoandrosta-1,3,5(10)-triene-9,17-dione, an intermediate in the microbiological degradation of ring A of androst-4-ene-3,17-dione. *The Journal of biological chemistry*. **241**, 540-550
- 46 Yang, X., Dubnau, E., Smith, I. and Sampson, N. S. (2007) Rv1106c from *Mycobacterium tuberculosis* is a 3 β -hydroxysteroid dehydrogenase. *Biochemistry*. **46**, 9058-9067
- 47 Rahm, M. A. and Sih, C. J. (1966) Mechanisms of steroid oxidation by microorganisms. XI. Enzymatic cleavage of the pregnane side chain. *The Journal of biological chemistry*. **241**, 3615-3623
- 48 Savvi, S., Warner, D. F., Kana, B. D., McKinney, J. D., Mizrahi, V. and Dawes, S. S. (2008) Functional characterization of a vitamin B12-dependent methylmalonyl pathway in *Mycobacterium tuberculosis*: implications for propionate metabolism during growth on fatty acids. *Journal of Bacteriology*. **190**, 3886-3895
- 49 Fryzuk, M. D. and Bosnich, B. (1979) Asymmetric Synthesis - Preparation of Chiral Methyl Chiral Lactic-Acid by Catalytic Asymmetric Hydrogenation. *Journal of the American Chemical Society*. **101**, 3043-3049
- 50 Frigerio, M., Santagostino, M., Sputore, S. and Palmisano, G. (1995) Oxidation of Alcohols with O-Iodoxybenzoic Acid (Ibx) in DmsO - a New Insight into an Old Hypervalent Iodine Reagent. *Journal of Organic Chemistry*. **60**, 7272-7276

Table 1: Comparison of different *meta*-cleavage hydrolases

Enzyme name	Organism	% sequence identical to HsaD	Highest temperature with 100% enzymatic activity (°C) ^a	Reference
ThnD	<i>Sphingomonas macrogoltabidus</i> strain TFA	26	65	[41]
BphD	<i>Rhodococcus</i> RHA1	29	65	[40]
CarC	<i>Pseudomonas</i> CA10	23	58	[42]
CumD	<i>Pseudomonas fluorescens</i> IP01	31	47.5	[44]
TodF	<i>Pseudomonas putida</i>	32	45	[43]

^aDifferent assay methods were used in different studies. This value represents the highest temperature the protein tolerated before enzymatic activity began to decrease

Figure 1: The NAT operon in *M. tuberculosis*.

The accession numbers for these genes in *M. tuberculosis* H37Rv, are as follows: *Rv3570c* (*hsaA*), *Rv3569c* (*hsaD*), *Rv3568c* (*hsaC*), *Rv3567c* (*hsaB*), *Rv3566A* (possible pseudogene) and *Rv3566c* (*nat*). The operon is virtually identical in *Mycobacterium bovis* and *Mycobacterium bovis* BCG.

Figure 2: Proposed pathway of cholesterol metabolism

Pathway of cholesterol catabolism as proposed by Sih *et al.* [45], Horinouchi *et al.* [22] and Van der Geize *et al.* [15]. There are two pathways of cholesterol degradation that proceed independent of each other. The first pathway is the degradation of the C17 acyl chain which produces two molecules of *n*-propionyl CoA and one molecule of acetyl CoA, per molecule of cholesterol. The second pathway is the degradation of the four ring cholesterol skeleton and has been linked to the *hsa* gene products.

Figure 3: CoA donor profile for recombinant purified TBNAT

The activity of TBNAT was determined by measuring the rate of CoA formation in the presence of hydralazine as described in the methods. The rate of CoA formation by TBNAT (0.75 µg) was measured in the presence of 500 µM hydralazine and various acyl CoA species (400 µM) in assay buffer (20 mM Tris-HCl, pH 8.0) with 0.5% DMSO at 37°C. The specific activity was determined over a linear range and is expressed as nmol of acyl coenzyme A hydrolysed sec⁻¹ mg of protein⁻¹.

Figure 4: Purification of HsaD

P. putida containing pVLT31-*hsaD*_H6 (lysate) was lysed and run through nickel-NTA resin (unbound). The column was then subsequently washed with increasing concentrations of imidazole (25-250 mM) in stepwise increments. A sample of each fraction (5 µl) was run on a 12% acrylamide SDS-PAGE and stained with Coomassie blue.

Figure 5: The effect of heat on NAT activity.

The NAT enzymes (**6A**: TBNAT **6B**: MMNAT, MM12TB3, TB12MM3) were incubated at increasing temperatures for 30 min, cooled on ice for 5 min, centrifuged for 10 min at 12,000 x *g* and then assayed for activity by following the hydrolysis of acetyl CoA in the presence of the substrate hydralazine. The specific activity was determined over a linear range. Each sample was performed in triplicate, the mean value is represented in the above graph ± standard deviation.

Figure 6: The effect of temperature on HsaD

A. The effect of heat on enzymatic activity was determined by incubating 160 µl of HsaD (0.5 mg/ml) in 100 mM sodium phosphate buffer pH 7.4 at 30-85°C for 30 min. The samples were then placed on ice for 5 min, centrifuged for 10 min at 12,000 x *g* and then assayed for activity. Each sample was performed in triplicate and the mean value ± standard deviation is shown. The circular dichroism of the protein (5 µM) was collected on a Jasco J720 spectropolarimeter at temperatures between 30-85°C (as determined by the sample probe).

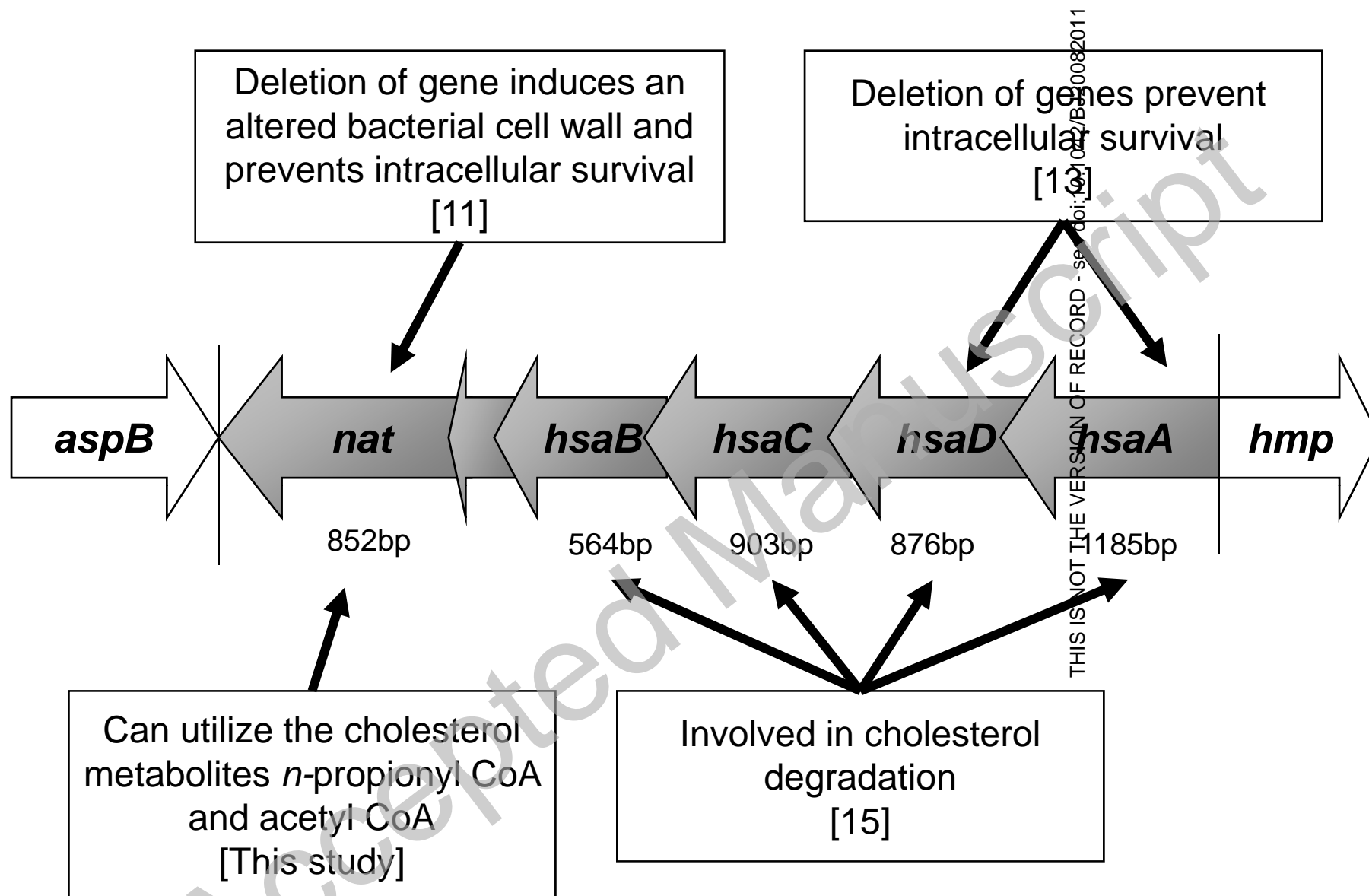
- B.** A sample of 5 μ M HsaD in 100mM phosphate buffer pH 7.4 was incubated at 65.8 \pm 0.4 $^{\circ}$ C (as determined by the sample probe) for 50 minutes. Every 300 seconds, the circular dichroism of the sample was measured (Applied Photophysics).
- C.** HsaD (160 μ l, 0.5mg/ml) in 10mM sodium phosphate buffer (pH7.4) with 0, 10, 50, 100 and 200mM NaCl was incubated at temperatures from 40-85 $^{\circ}$ C for 30min. Following incubation, the samples were assayed for activity. For clarity only the samples with 0 and 200mM NaCl are shown. All other concentrations of NaCl display a similar trend.

Figure 7: Amino acid differences between MMNAT and TBNAT in domain one and two

- A.** NAT protein ClustalW alignment of domain one and two from MMNAT, MSNAT and TBNAT. Amino acids which are identical in MMNAT and MSNAT, yet differ from TBNAT are highlighted by an arrow. Active site residues are shown with a star. Only domain one and two are shown as domain three does not appear to strongly contribute to the protein's heat stability.
- B, C and D.** Cartoon (**B**) and surface (**C,D**) representation of the amino acid sites which differ between MMNAT/MSNAT and TBNAT displayed on the crystal structure of MMNAT (PDB: 2VFB). Domains one and two of the MMNAT are shown as blue, while domain three is shown as white. The active site residues are shown as green, and the amino acids which differ between the MMNAT/MSNAT and TBNAT are shown in red and labelled. In figure **B** all highlighted amino acids are displayed in stick representation. The view in **D** is rotated through 180 degrees in the vertical plane compared with view **C**.

Figure 8: Comparison of meta-cleavage hydrolases

- A.** ClustalW alignment of the meta-cleavage hydrolases from *Pseudomonas fluorescens* IP01 (CumD), *Pseudomonas putida* F1 (TodF), *Sphingomonas macrogoltabidus* strain TFA (ThnD), *Rhodococcus* RHA1 (BphD), *M. tuberculosis* H37Rv (HsaD) and *Pseudomonas* CA10 (CarC).
- B.** Structural alignment of meta-cleavage hydrolases. CumD is shown in white, BphD is shown in dark grey, CarC is shown in light blue and HsaD is shown in dark blue. The active site (Ser-Asp-His) of HsaD is shown in green.

**Figure 1**

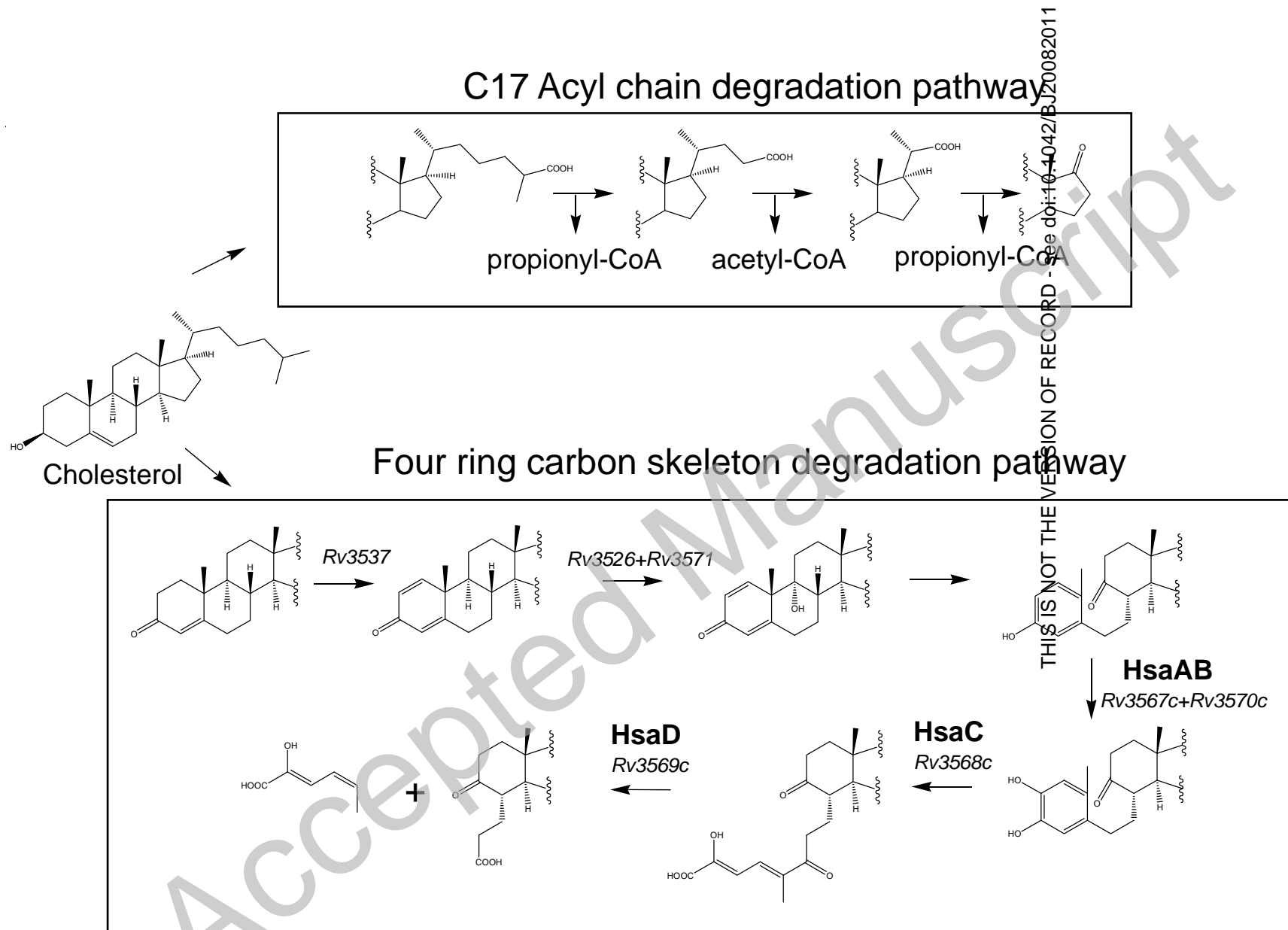


Figure 2

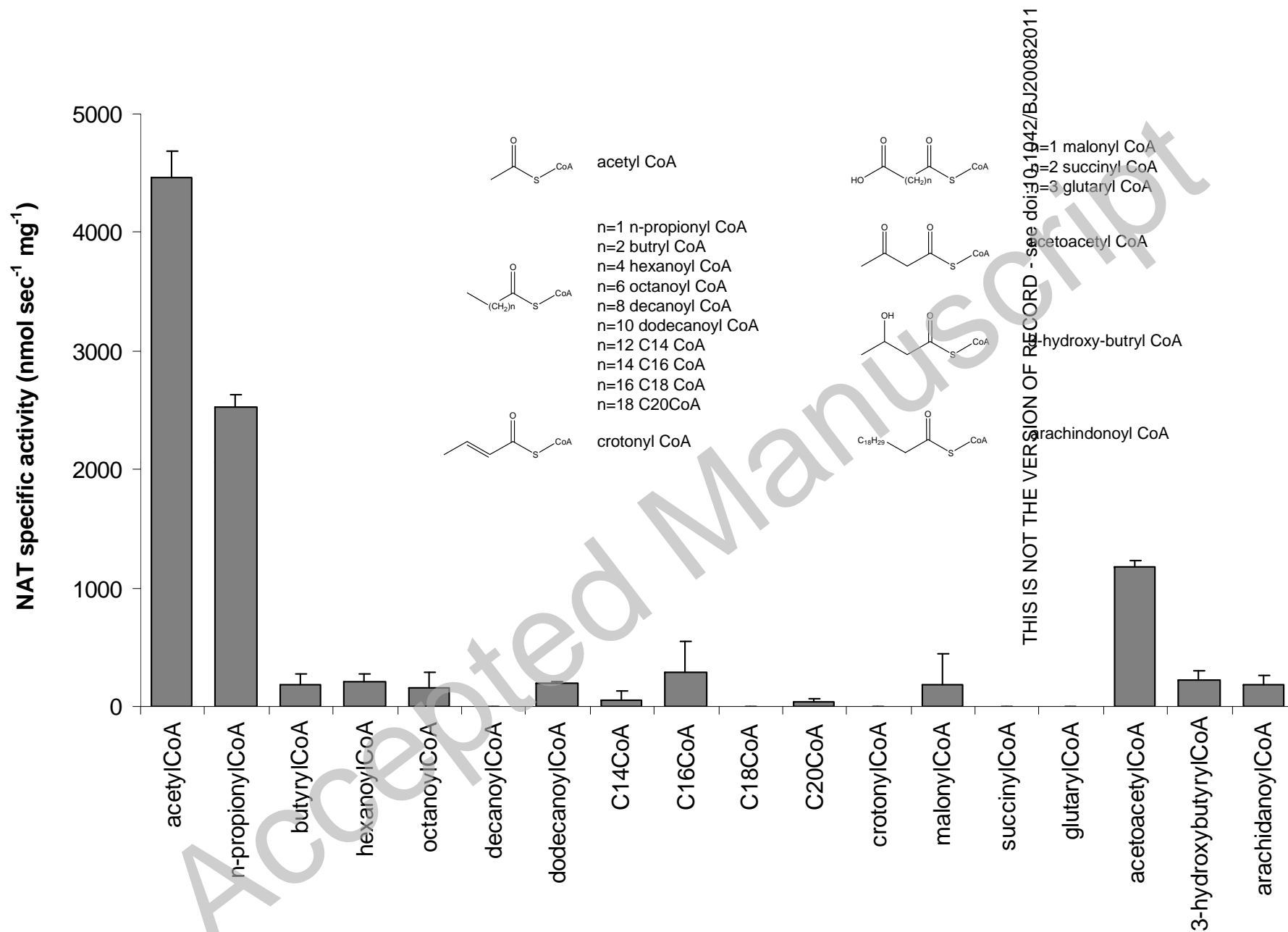


Figure 3

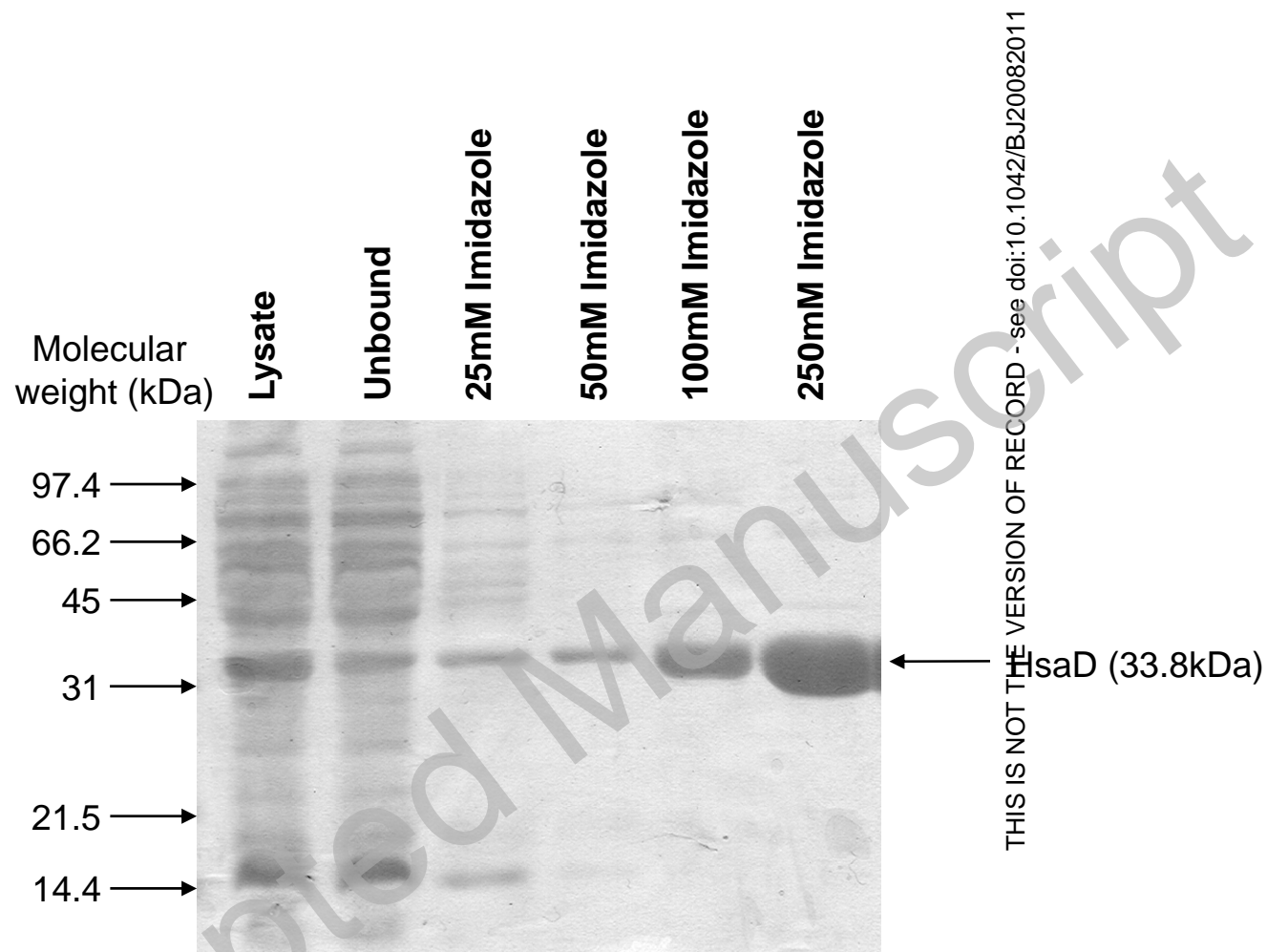


Figure 4

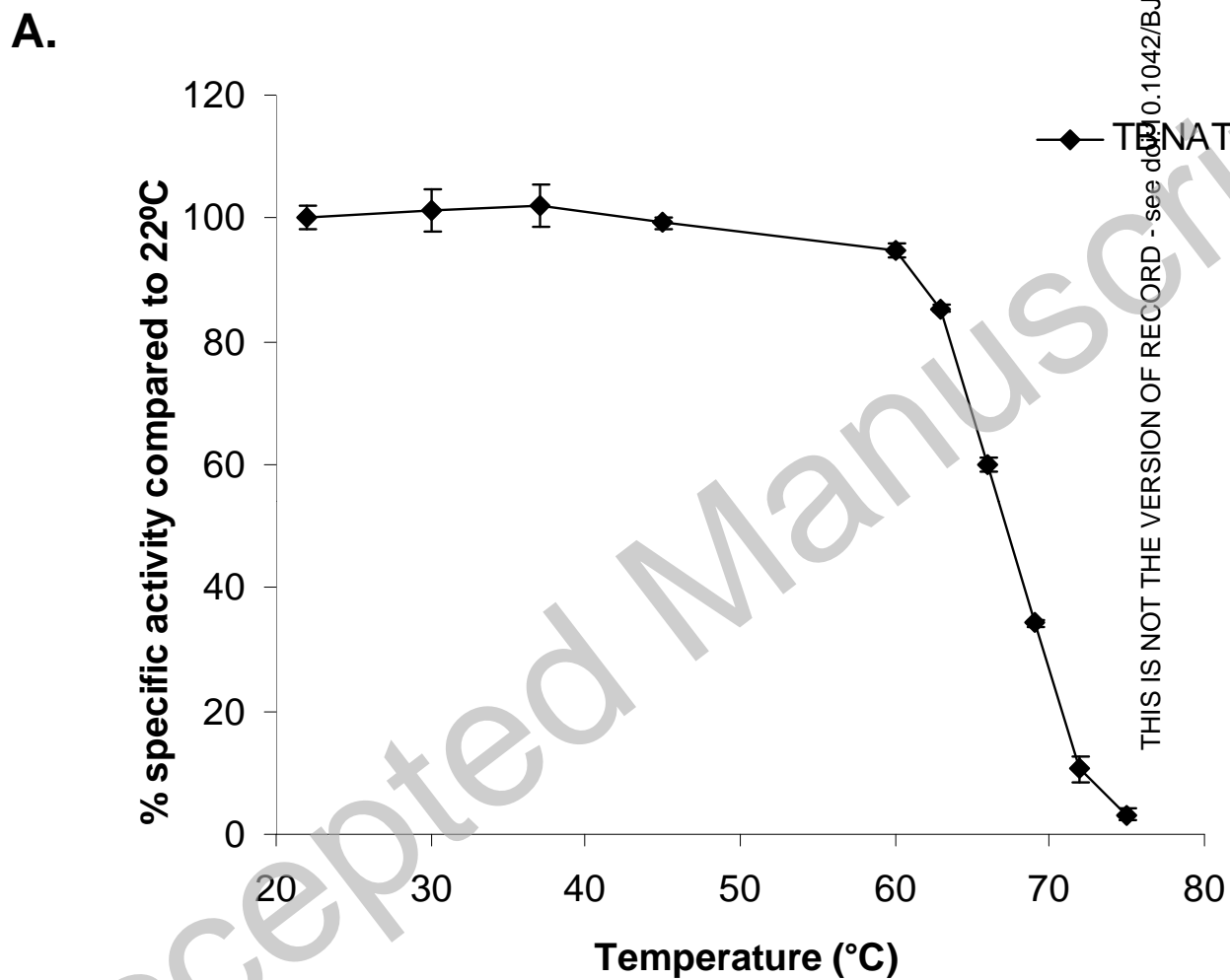
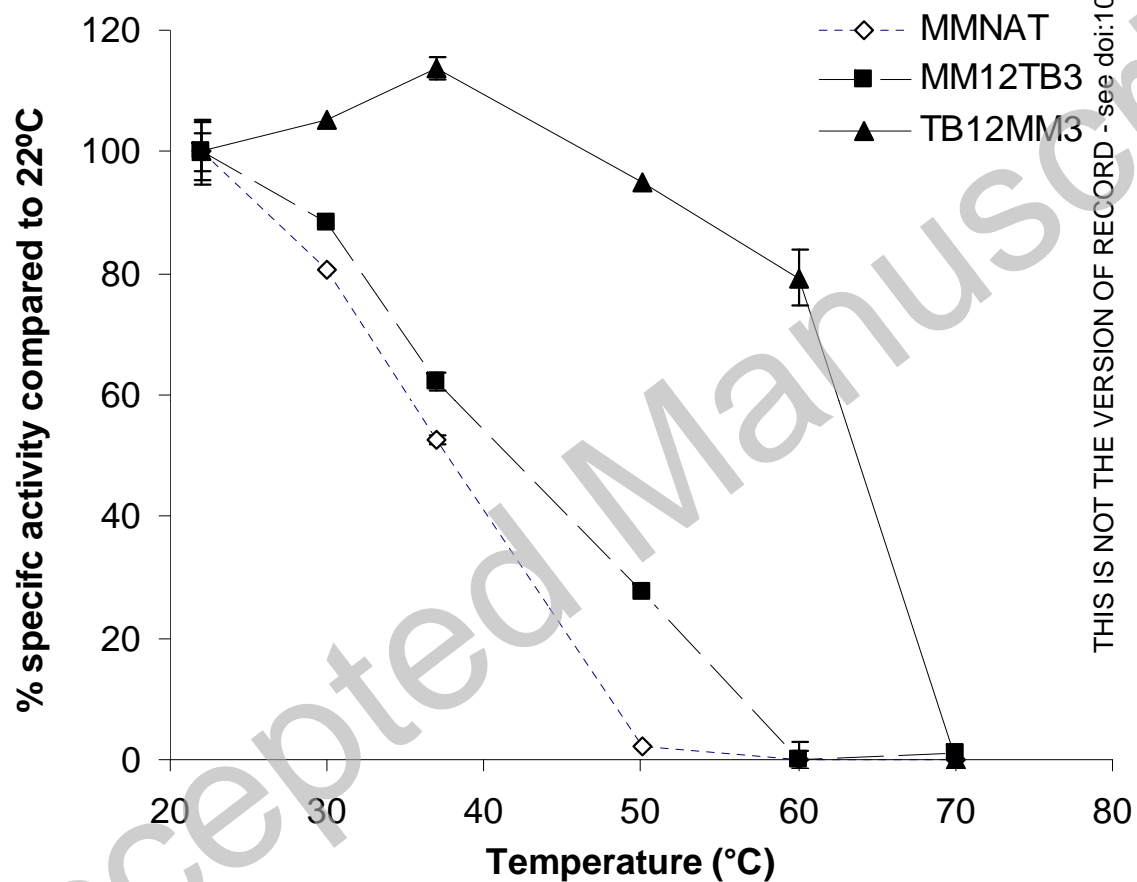


Figure 5

B.



THIS IS NOT THE VERSION OF RECORD - see doi:10.1042/BJ20082011

Figure 5

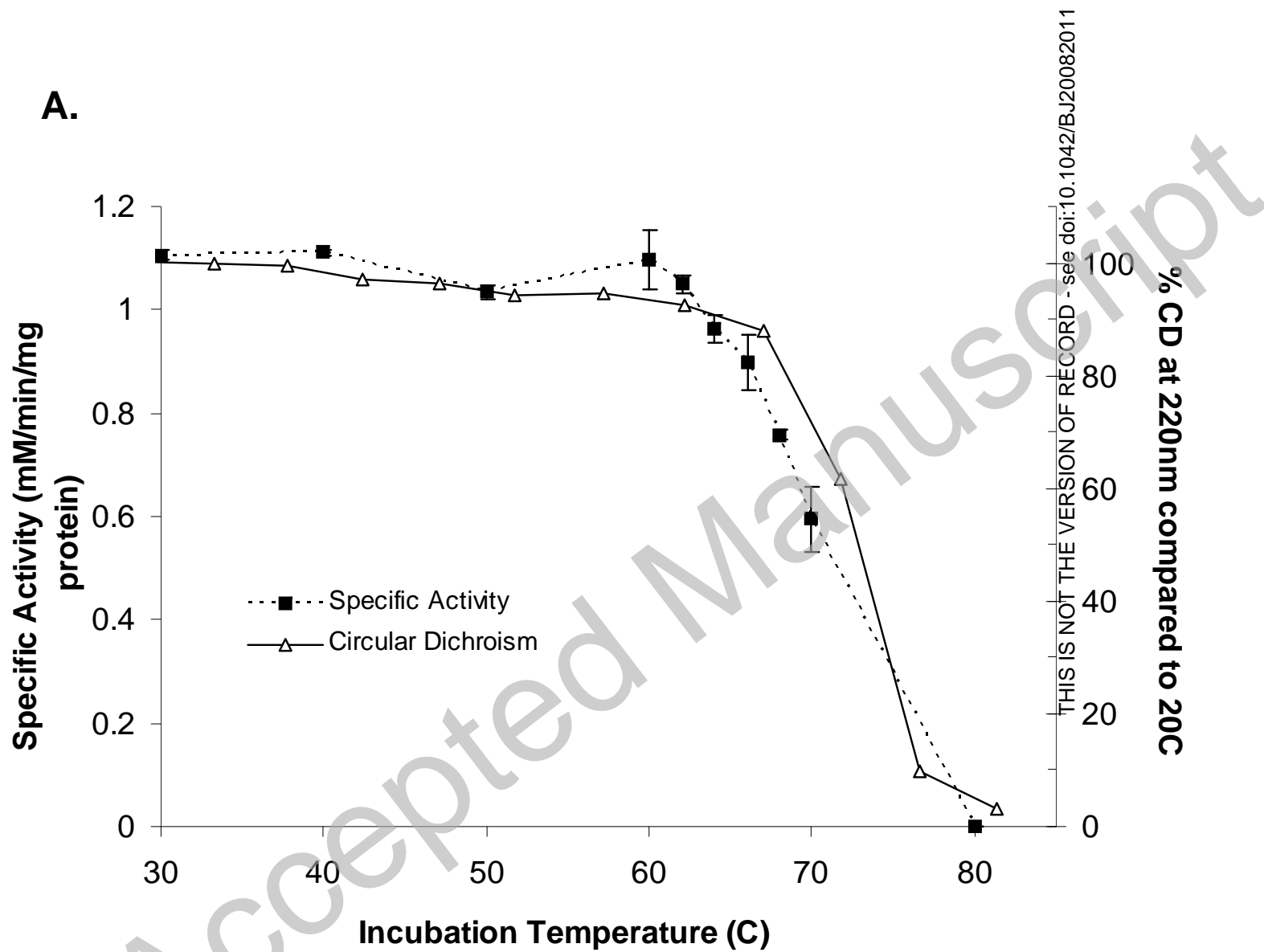


Figure 6

B.

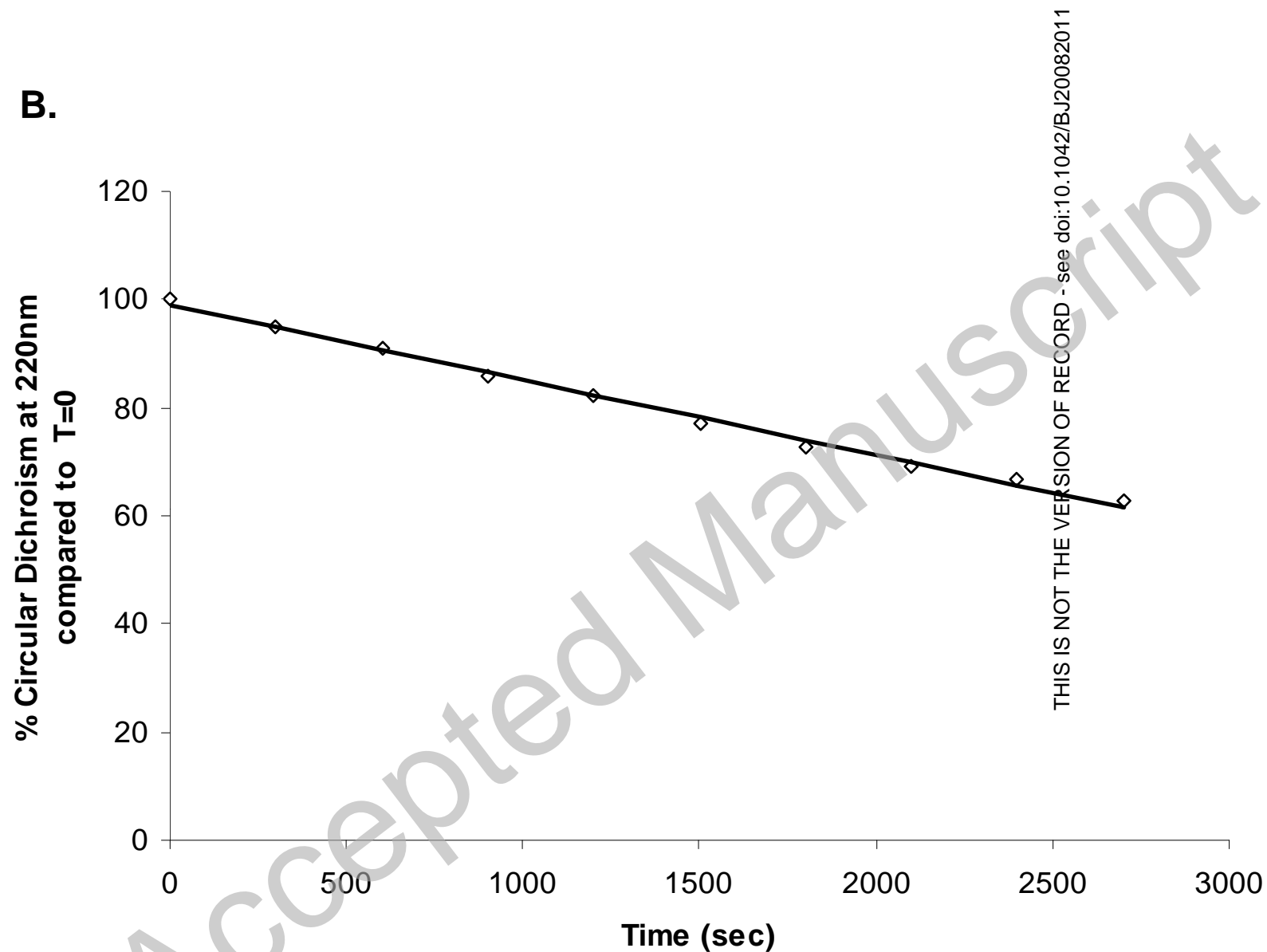
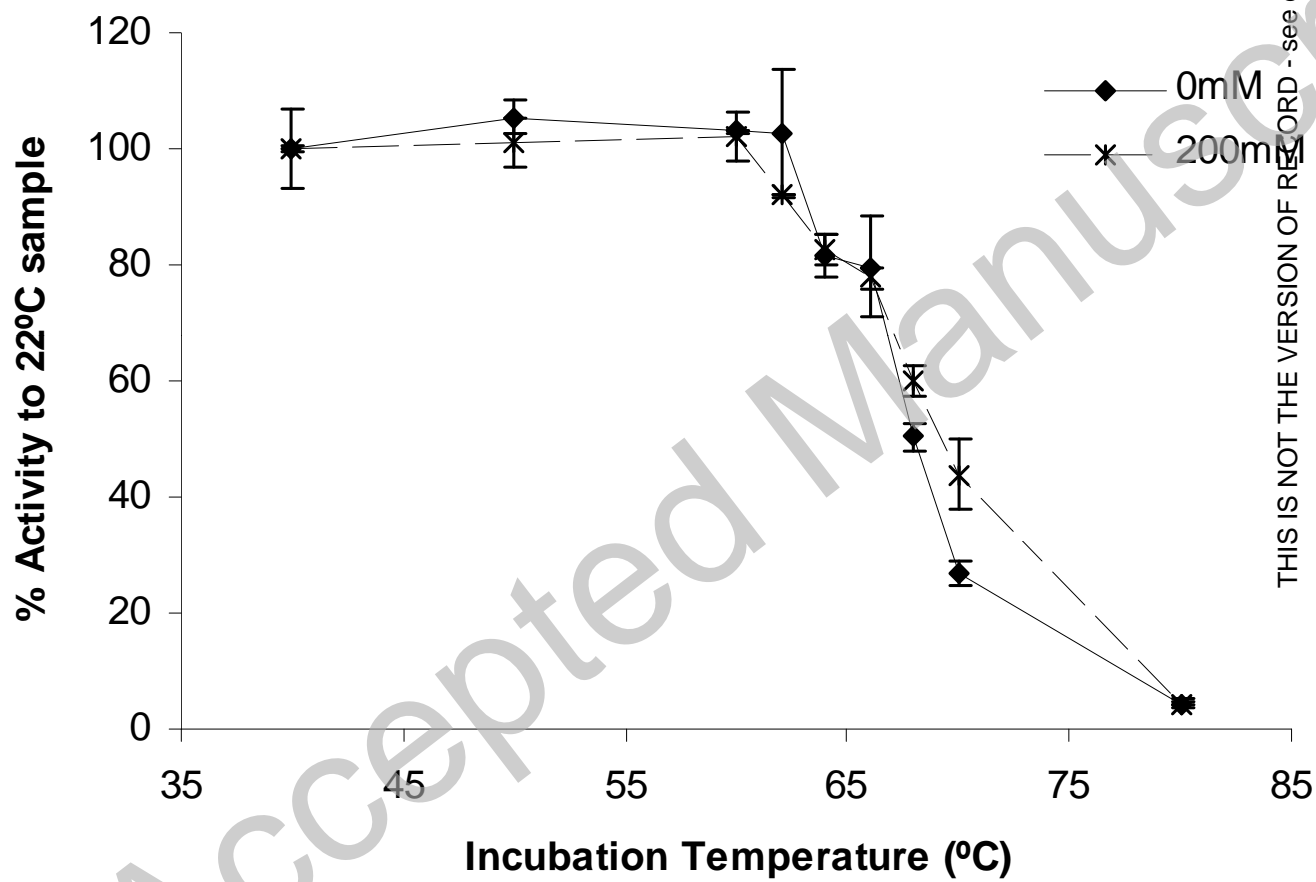


Figure 6

C.



THIS IS NOT THE VERSION OF RECORD - see doi:10.1042/BJ20082011

Figure 6

A.

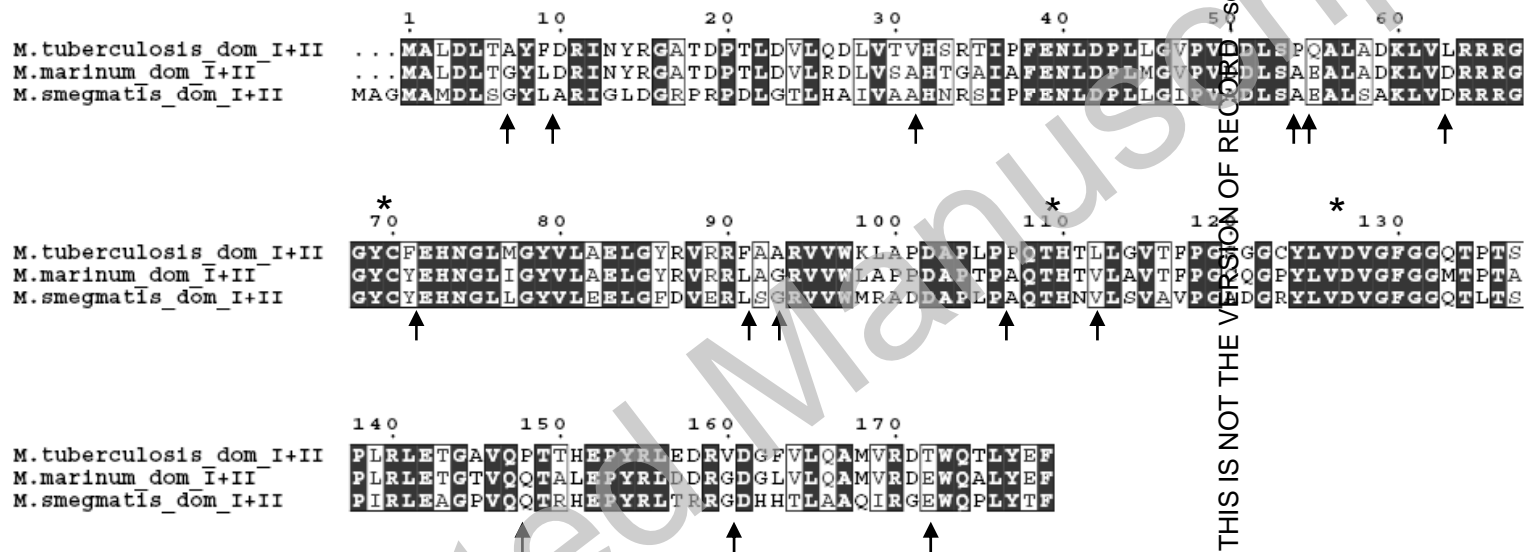
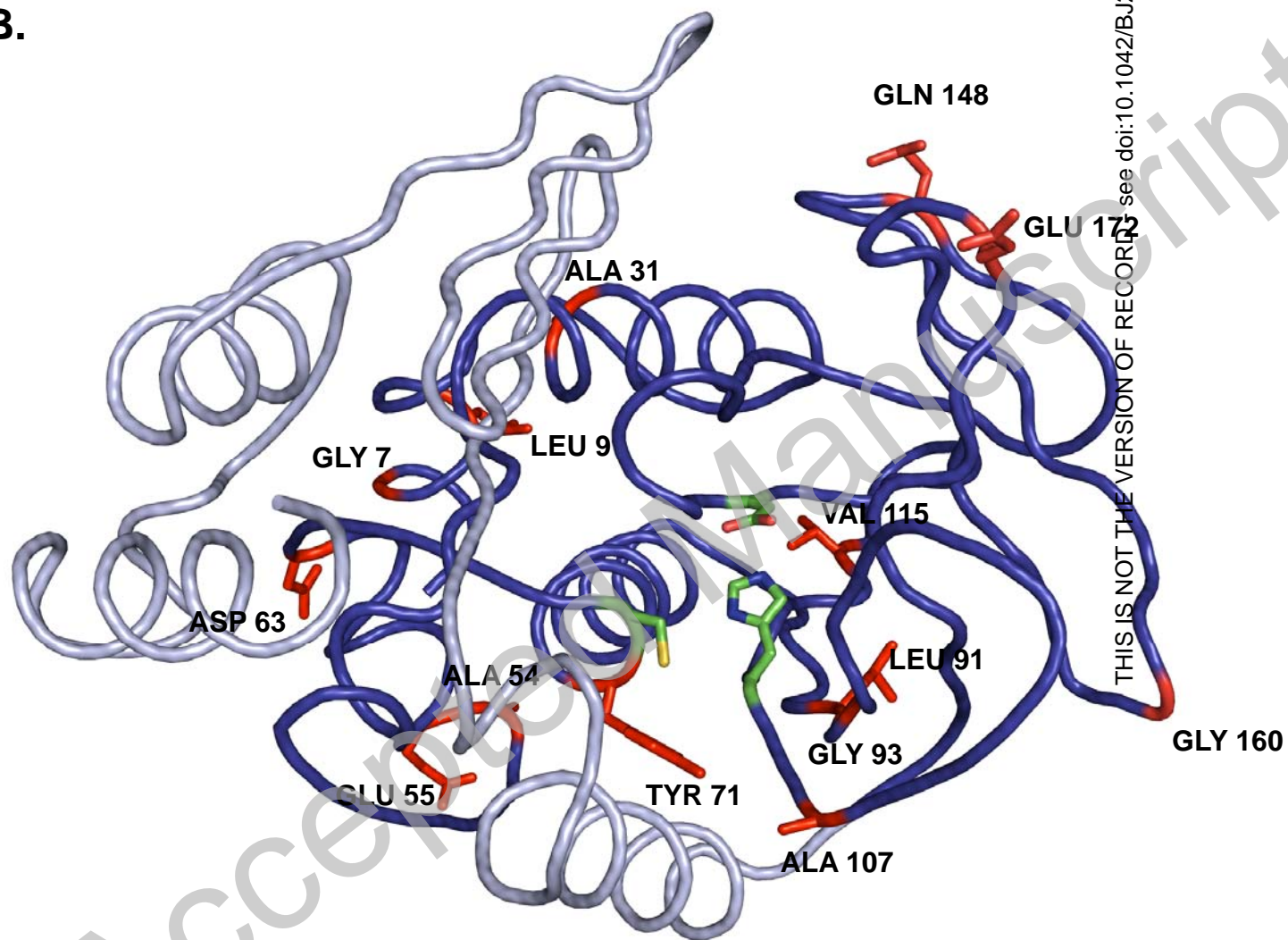
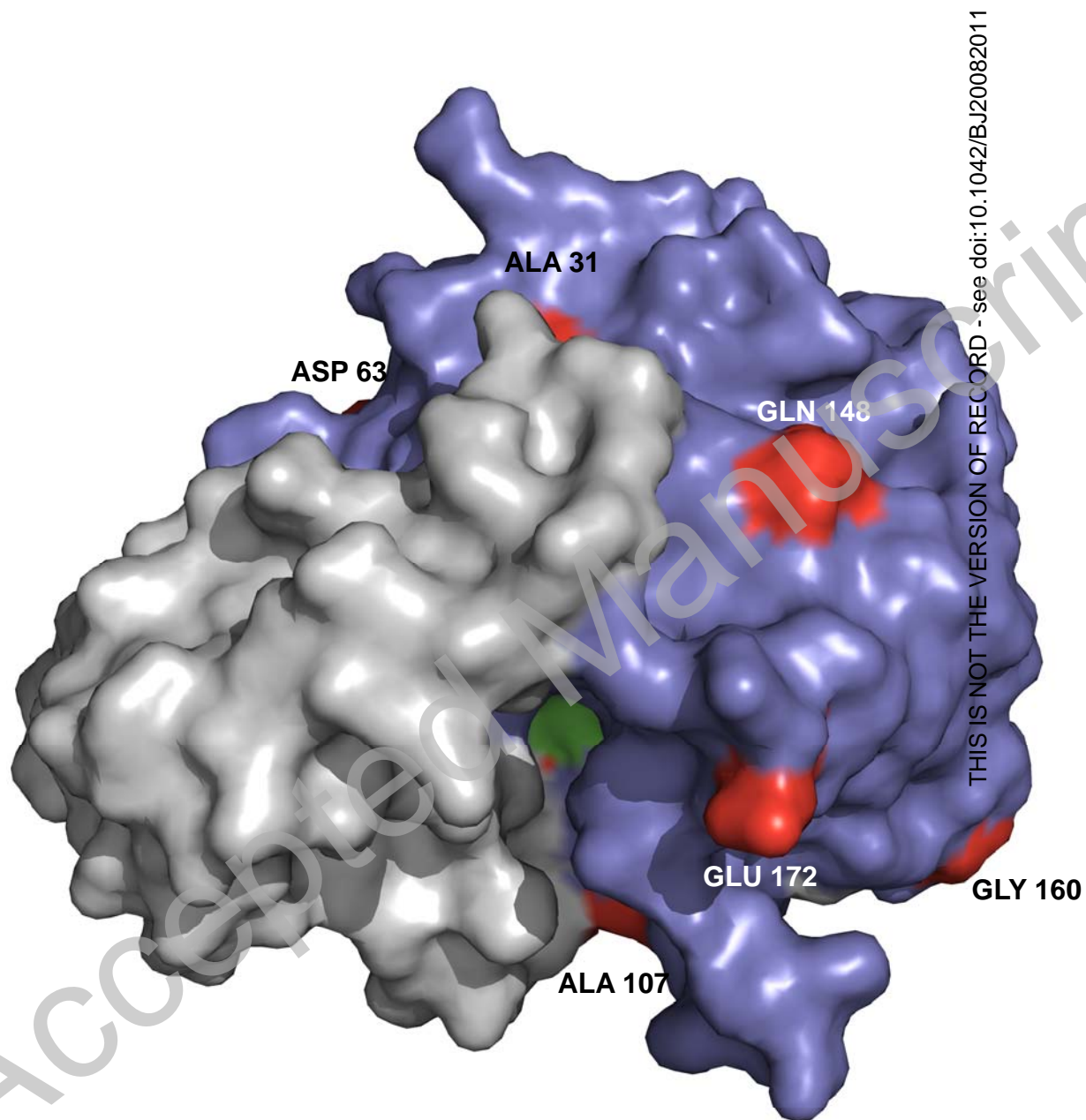
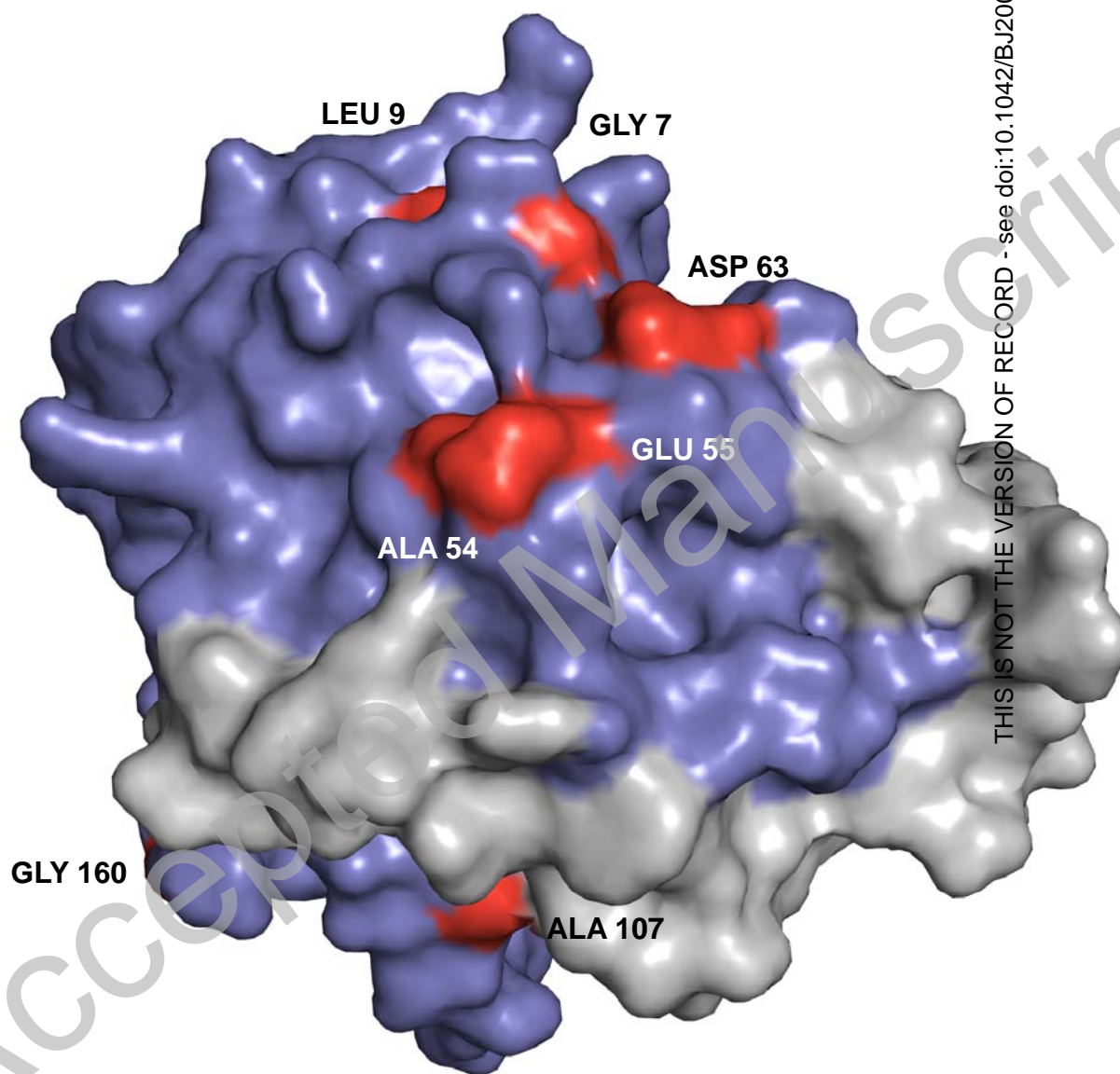


Figure 7

B.**Figure 7**

C.**Figure 7**

D.



THIS IS NOT THE VERSION OF RECORD - see doi:10.1042/BJ20082011

Figure 7

A.

```

1          10          20          30          40          50
CumD_Pseudomonas fluorescens I ...MANLEIGKSIIL.....AAGVLTNYHDVGGQ...PVILIEGSGPGVSA...MRLTIPALSKFTFV
TodF_Pseudomonas putida F1    .MTNVNAEIGRMVWL.....AGGIETNLHDVQAGN..PVVLLVHGSGPGVTAK...MRTVMPPLSRHFRV
ThnD_Sphingomonas macrogoltabi .MSEAFVVEKRLP.....TKPYETHVMIGGDPANPPLL...LVHGARPGGSA...MTRHCFADLVKDFYV
BphD_Rhodococcus EHA1       .MAKTVEIIEKRFPP.....SGTLASHALVAGDPQSPAVVLLHGAGPGAA...MTRPIIEDLAENRFV
HsaD_Mycobacterium tuberculosis .MTATEELTPESYTSRFAEVDV.DGPLKLLHYHEAGVNDQTVVLLHGSGPGAA...MTRPIIEDLAENRFV
Carc_Pseudomonas CA10       MLNKAEOISEKSESAYVERFVNAGGVETRYLEAKGQ...PVILIEGSGGAGSE...MTRNVIPIIARHFRV

60          70          80          90          100         110         120
CumD_Pseudomonas fluorescens I IAPDQVGGPGPTDR...PENYNYSKDSWVDH...IGTMDALETE..KAHIVGNSP...GATATALRYSERVDR
TodF_Pseudomonas putida F1    IAPDQVGGPGPTQR...PHGIHYGVESWVAHLAGILDALDLD..EVDVWNSG...GSLAFAIRPFFHFRV
ThnD_Sphingomonas macrogoltabi IAPDQVGGPGQSEIPDPVPAHAVTWMGLRIEQAFGVLDLGLIE..KTHIVGNS...GALHMLMEQDPRFDK
BphD_Rhodococcus EHA1       VAPDLICFGQSEYTPETYPGHIMSWVGMRV...EQILGLMNEPGIE..KSHIVGNS...GGLVTLQVVEAPERFDK
HsaD_Mycobacterium tuberculosis IAPDQVGGPGHSDK...RAEHGQFNRYAAMALKGLFDQGLG..KVPVIVGNS...GGLTAVRPAIDYPARAGR
Carc_Pseudomonas CA10       IAMDMLGGPKTAKP....DIEYTTQDRRI...RHLDDELKAMHEDGKY...IVGNS...GGLGGLVSVLHSELVNA

130         140         150         160         170         180
CumD_Pseudomonas fluorescens I MVLMGRAAGTRPFDVTEG.....LNAVWGYTPE...ENMENLDDIPAYERSLVT...ELARLEYEASTIQPGF
TodF_Pseudomonas putida F1    LVLMGRAAGVSPFLTDG.....LDNAVWGYE...SVNMRVMDYFAYERSLVS...ELALEYETKASTRPGF
ThnD_Sphingomonas macrogoltabi VMTMGPAKMDATP...ELVDELVNFYADPRLPRYREVINSPVY...PSLVPNL...EITQERFKIATDPEV
BphD_Rhodococcus EHA1       VALMGVVGAPMNAKRP...ELALALAFYADPRLTPYREL...LIHSPVY...DENPPGM...SIVKSRFEVANDPEV
HsaD_Mycobacterium tuberculosis LVLMGFGGLSINLFPAPDTEGV...ELKLSKFSVAP...THENLEAPLRVMVY...DKNLIT...PELVDCRPAI...ASTPES
Carc_Pseudomonas CA10       LVLMGSAGLVWV...RHED...LSPIN...YNDP...TEG...MVLV...KAL...ND...GPKID...L...AMINS...RYTYA...TDEAT

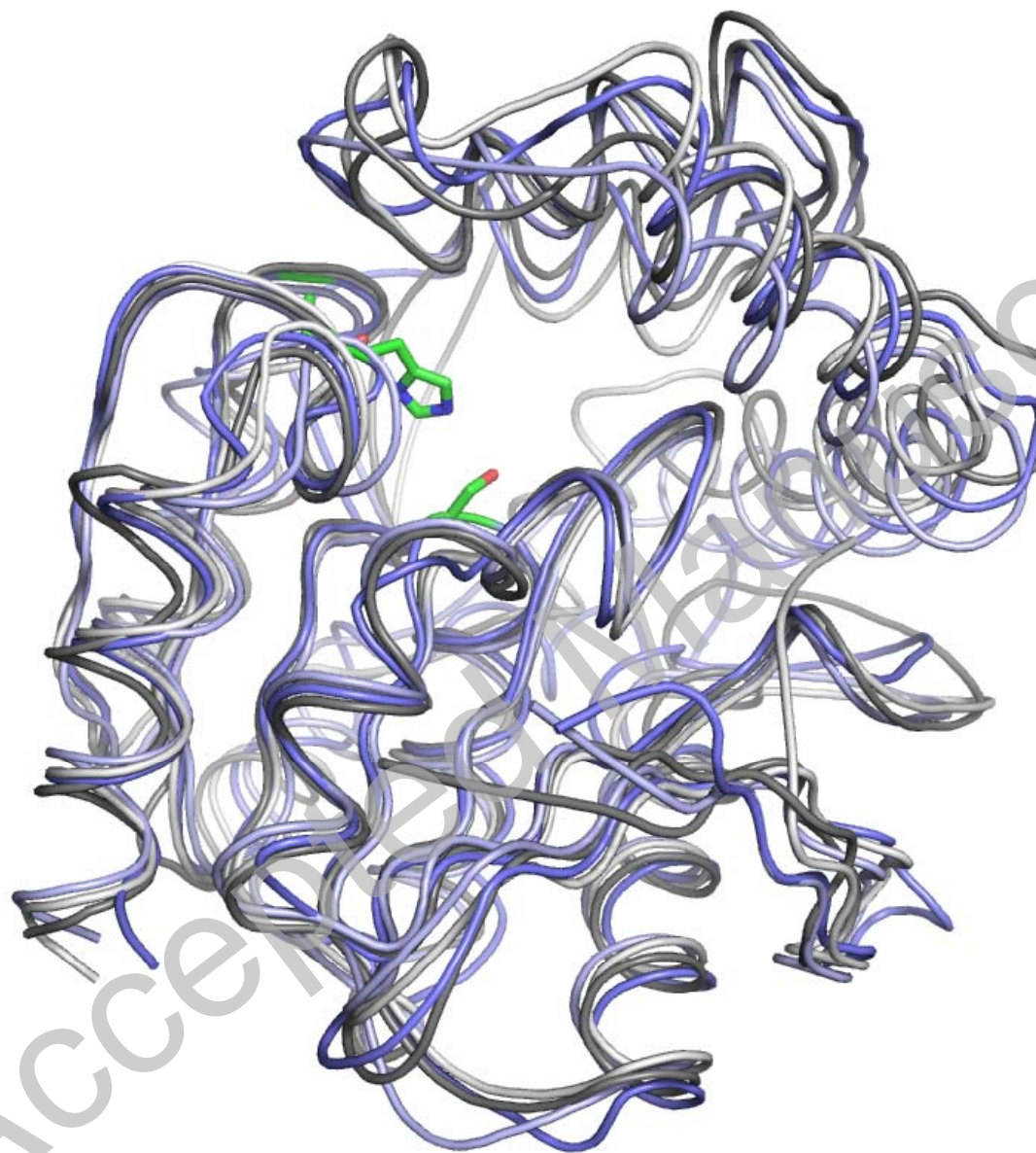
190         200         210         220         230         240         250
CumD_Pseudomonas fluorescens I QESFSSMFPPEPRRWIDALASSDEDIKTL...PNETLI...IHGR...EDQVVP...LSS...SLRLG...EDRAQLHV...FGR...CGHW
TodF_Pseudomonas putida F1    QEAFA...SMFP...PAP...QRWVDALASSDQ...DIR...DIRHET...LILHGR...DDREVI...PLET...SLRLNQL...IEP...QLHV...FGR...CGHW
ThnD_Sphingomonas macrogoltabi RRVQEVMPES.MITGMPALVVPPSALKRIPHEVALVHGRH...DEVI...PLQASLYLLEHLQRAELFVLDRC...GHW
BphD_Rhodococcus EHA1       RRIQEVMPES.MIAGMESLVIPPATLGRLLPHDVLVPHGR...QDRIV...PLDTS...LYLTKHLKHAELVWLDRC...GHW
HsaD_Mycobacterium tuberculosis DTATRAMGKS.PAGADPEAGMMWR...VRLRQ...VLL...LWGR...EDRVN...PLD...GALVALK...TIPRAQLHV...FGR...CGHW
Carc_Pseudomonas CA10       RKAIVATMQWIREQG...GLFYDPE...PRK...VVPV...LVVH...GND...KVV...VETAY...KFLDL...IDD...NGY...IIP...H...CGHW

260         270         280
CumD_Pseudomonas fluorescens I TQIEQTD...RPNR...LVVEFFNEANTPKLVGRP
TodF_Pseudomonas putida F1    VQIEQNRGFI...RLVNDFLAAED.....
ThnD_Sphingomonas macrogoltabi AQIQ...RNDAMLP...IERNHFLETAR.....
BphD_Rhodococcus EHA1       AQLERNDAMGEMLM...EHFRAA.....
HsaD_Mycobacterium tuberculosis VQVEKPFDEFNKLTIEF...LGGGR.....
Carc_Pseudomonas CA10       AMIEHPEDPANATLSPLSR...RADITRAAA.

```

THIS IS NOT THE FINAL VERSION OF THIS RECORD - see doi:10.1042/BJ20082011

Figure 8

B.

THIS IS NOT THE VERSION OF RECORD - see doi:10.1042/BJ20082011

Figure 8